Unified theory of Raman and parametric amplification in nonlinear microspheres

M. V. Jouravlev* and G. Kurizki†
Department of Chemical Physics, Weizmann Institute of Science, 76100, Rehovot, Israel
(Received 21 June 2004; published 4 November 2004)

We investigate the scattering threshold and cavity-enhanced gain in nonlinear spheres with second- or third-order permeability. Pairs of pump-driven idler and signal modes are considered, satisfying morphology-dependent resonance conditions. The thresholds and gain coefficients of amplified and stimulated Raman scattering, parametric downconversion, and analogous parametric processes in microspheres are derived and evaluated under typical conditions. Applications may include the measurement of chemical impurity concentrations or the creation of low-threshold optical parametric amplifiers using microspheres.

DOI: 10.1103/PhysRevA.70.053804 PACS number(s): 42.50.Dv, 42.60.Da

I. INTRODUCTION

Raman scattering and parametric generation of electromagnetic waves by a transparent dielectric sphere have long been subjects of both fundamental and applied interest in nonlinear optics [1–8]. On the fundamental side, they provide examples of parametric amplification or harmonic generation that are determined by the spatial extent, boundary conditions, and symmetry of the medium. On the applied side, spectral analysis of stimulated Raman scattering and other types of inelastic radiative scattering (or parametric generation) by microspheres is a powerful means of gaining information about their size, chemical composition, and impurities concentration and may be used for aerosol particle identification. Yet quantitative evaluation of the spectra of such inelastic scattering is challenging, because the radiation field within the microparticle depends in a complicated way on its size, refractive index, and wavelength, at wavelengths near the morphology-dependent resonances (MDR's), also known as Mie scattering resonances [1,2]. Parametrically amplified scattering from microspheres is associated with two types of resonances: MDR's of the incident wavelengths, known as input resonances, and resonances of the inelastically scattered light, known as output resonances [3]. MDR's have been observed in the Raman spectra of spherical aerosol particles and droplets [4,5].

The experimentally observed drastic reduction of the threshold pump intensity for spontaneous Raman scattering from micrometer-size droplets has been attributed to cavity quantum electrodynamic effects under the input-output resonance condition [5,6]. Cavity-enhanced fluorescence and stimulated Raman scattering under input resonance conditions were first explained by introducing the spatial overlap of interacting mode functions in the equations of stimulated scattering in Ref. [7]. It is well established that spherical liquid droplets undergoing laser irradiation exhibit threshold behavior for stimulated and spontaneous Raman scattering that requires spatial overlap between the interacting partial modes [8]. By contrast, the analog of phase-matching conditions [4,9] in spheres requires further consideration.

In this article we develop the theory of microcavity-enhanced Raman or parametric generation gain and calculate the thresholds of spontaneous and stimulated (coherent) Raman or parametric amplification for nonlinear dielectric spheres with large MDR orders. To this end, previously suggested approaches [10,11] are further developed to render the explicit dependence of the gain and threshold on experimental parameters. The present calculation involves the eigenfrequencies and electromagnetic modes of a sphere and their spatial overlap. The general formulas obtained here for the threshold and gain are valid in a resonator of any shape. However, for each shape it is necessary to know the appropriate solution of the problem of diffraction by the dielectric resonator and to obtain its eigenfunctions from the boundary conditions. Analytical solutions for spherical eigenmodes [2,12], which have been extensively investigated in the past decade [13], are used here to obtain closed-form expressions for the gain spectrum and the threshold conditions.

We are concerned with dielectric spherical media with quadratic, $\chi^{(2)}$, or cubic, $\chi^{(3)}$, nonlinear susceptibilities. A simplified model of two interacting modes satisfying both the input and output resonant conditions may be used to evaluate the threshold intensity and gain for parametric amplification or for Raman conversion of a pump into a Stokes field. In general, an infinite number of modes will be coupled in such a spherical resonator. However, we may ignore all but the two nondegenerate modes with the highest Q factors and largest intermode coupling coefficients, obtainable from either experimental or numerical data [14–17].

The most crucial variable describing the interaction of light with a dielectric microsphere is the size parameter $\rho = ka$, where a is the radius of the sphere and k is the wave number in the dielectric medium. The interest lies principally with input resonance conditions such that the laser pump (or idler) and the Stokes (or signal) modes both correspond to high-Q modes of the cavity [5,16]. When the size parameter satisfies the equation of $\rho \simeq n$, n being a large integer, the scattering exhibits a complicated angular pattern due to interference among many partial waves and has sharp peaks, corresponding to nth-order MDR's [17]. Such resonances can be extremely narrow, with Q factors as high as 10^8 for perfectly round, homogeneous, and transparent silica spheres

*Also at Karpov Institute of Physical Chemistry, Vorontsovo Pole 10, 103064, Moscow, Russia.
†Electronic address: gershon.kurizki@weizmann.ac.il

[18] and spherical aerosol droplets [19]. The highest-Q MDR's, whose electromagnetic energies are concentrated in a narrow surface layer [20], governs the nonlinear properties. Special attention in our calculations is paid to the dependence of the threshold intensity and enhanced Raman gain upon the MDR orders. Enhancement of the Raman scattering is explained here by the Raman power integrated over the MDR volume, as determined by the characteristics of the mode-overlap integral.

This paper is organized as follows: in Sec. II we derive the basic expressions for threshold intensities and cavity-enhanced gain for Raman amplification and for parametric downconversion under input and output resonance conditions, as well as the functional dependence of Raman gain on the active molecules concentration. In Sec. III we describe the implementation of these expressions in typical cases and the pertinent numerical calculations. In Sec. IV we discuss the results of the calculations and predict the decrease of the threshold pump intensity when the parametric interaction of surface modes takes place. We then survey some possible applications of these results and summarize our conclusions in Sec. V. The Appendix provides explicit formulas for the spherical mode eigenfunctions and MDR frequencies used in the text.

II. BASIC EXPRESSIONS FOR THRESHOLD AND GAIN

A. Hamiltonians

The interactions between modes in a nonlinear cavity are described by the field-interaction Hamiltonian density in the form of [21,22]

$$H_{int} = -\frac{2}{3}\sum_{ijk} \chi^{(2)}_{ijk}\vec{E}_i\vec{E}_j\vec{E}_k \tag{1}$$

or

$$H_{int} = -\sum_{ijkl} \chi^{(3)}_{ijkl}\vec{E}_i\vec{E}_j\vec{E}_k\vec{E}_l, \tag{2}$$

where i, j, k or i, j, k, l indicate three or four interacting partial waves. Because of the energy conservation condition, the fields $\vec{E}_i$, $\vec{E}_j$, $\vec{E}_k$, and $\vec{E}_l$ in Eqs. (1) and (2) are centered at cavity eigenfrequencies satisfying $\omega_i+\omega_j=\omega_k$ or $\omega_i+\omega_j=\omega_k+\omega_l$, respectively. The coefficients $\chi^{(2)}_{ijk}$ and $\chi^{(3)}_{ijkl}$ are the corresponding effective nonlinear susceptibilities. The electromagnetic fields inside the cavity can be quantized as

$$\vec{E}(\vec{r},t) = -\sum_j i\left(\frac{\hbar\omega_j}{2\varepsilon_j}\right)^{1/2}[a_j^{\dagger}(t) - a_j(t)]\vec{E}_j(\vec{r}), \tag{3}$$

where $a_j^{\dagger}$ and a_j are the creation and annihilation operators for the jth mode and ε_j is the dielectric permeability. The TE and TM field eigenfunctions in Eq. (3) are the solutions of the Helmholz equations

$$\vec{\nabla}\times\vec{\nabla}\times\vec{E}_j(\vec{r}) + k_j^2\vec{E}_j(\vec{r}) = 0 \tag{4}$$

and

$$\nabla^2\vec{E}_j(\vec{r}) + k_j^2\vec{E}_j(\vec{r}) = 0, \tag{5}$$

respectively, obeying the cavity boundary conditions and satisfying the normalization condition within the cavity volume V:

$$\int_V \vec{E}_i(\vec{r})\vec{E}_j(\vec{r})dV = \delta_{ij}. \tag{6}$$

We shall quantize the Raman-amplified modes or those parametrically generated or amplified at frequencies ω_i, ω_j upon replacing $\vec{E}_i(\vec{r},t)$, $\vec{E}_j(\vec{r},t)$ by their corresponding quantum mechanical operators. By contrast, we shall treat the field mode excited by a laser pump classically and assume that it remains undepleted by the nonlinear interaction. This quantum approach is widely employed for parametric nonlinear processes in cavity electrodynamics [22].

After some standard manipulations, the Hamiltonians (1) and (2) for nonlinear interactions in the cavity may be cast in the energy-conserved form that consists of two parts [6,11,23,24]: (a) the part responsible for Raman scattering or coupling between the pump and the Stokes waves,

$$H_{Raman} = \hbar\sum_{i,j}\{S^{(n)}_{ij}a_i a_j^{\dagger} + \text{H.c.}\}, \tag{7}$$

and (b) the parametric amplification (PA) part responsible for parametric down-conversion (PDC) of the pump wave at ω_k into a sum of signal and idler waves or the inverse process (three-wave mixing) in $\chi^{(2)}$ media ($n=2$), satisfying $\omega_k=\omega_i+\omega_j$, and for four-wave mixing in $\chi^{(3)}$ media ($n=3$), satisfying $2\omega_k=\omega_i+\omega_j$:

$$H_{PA} = \hbar\sum_{i,j}\{(A_k^{n-1}S^{(n)}_{ij}a_i a_j + \text{H.c. }\}. \tag{8}$$

Here H.c. denotes Hermitian conjugation: $a\leftrightarrow a^{\dagger}$. The PA Hamiltonian (8) is proportional to the classical amplitude of the incident pump, A_k (taken to be real) in $\chi^{(2)}$ media ($n=2$) and A_k^2 (number of photons at ω_p) in $\chi^{(3)}$ media ($n=3$). In both Raman and PA Hamiltonians, $S^{(n)}_{ij}$ are the nth-order integral coefficients ($n=2$) or ($n=3$) of nonlinear coupling of the form [9,21,22]

$$S^{(2)}_{ij} = \frac{b_k(\omega_i\omega_j)^{1/2}}{6m^2}\chi^{(2)}_{ijk}\int_V \vec{E}_i(\vec{r})\vec{E}_j(\vec{r})\vec{E}_k(\vec{r})dV \tag{9}$$

for $\chi^{(2)}$ processes or

$$S^{(3)}_{ij} = \frac{b_k^2(\omega_i\omega_j)^{1/2}}{2m^2}\chi^{(3)}_{ijkk}\int_V \vec{E}_i(\vec{r})\vec{E}_j(\vec{r})\vec{E}_k(\vec{r})\vec{E}_k(\vec{r})dV \tag{10}$$

for $\chi^{(3)}$ processes. Here m is the refractive index and b_k is the partial-wave amplitude of the ω_k mode within the cavity (Mie-scattering solution) for either TE or TM modes [Eqs. (A5) and (A6)]. The Raman Hamiltonian terms (7) have the form $a_i^{\dagger}a_j$ and $a_i a_j^{\dagger}$, corresponding to the transfer of energy by single-photon exchange between the pump and Stokes fields, respectively. In Hamiltonian (8) the $a_i a_j$ and $a_i^{\dagger}a_j^{\dagger}$ terms correspond to two-photon emission or absorption into the signal and idler modes at the expense of the pump modes, known as parametric down-conversion in $\chi^{(2)}$ media. The properties of integral coefficients $S_{ij}^{(2)}$ and $S_{ij}^{(3)}$ are defined by selection rules derived from the theory of angular momentum (Sec. III) [25]. In what follows, we shall treat the Hamiltonians (7) and (8) separately.

B. Raman threshold and gain

In the case of the Raman Hamiltonian (7), upon substituting the photonic state $|\Psi\rangle = \Sigma_{n_i,n_j} C_{n_i,n_j} |n_i, n_j\rangle$, with n_i, n_j photon numbers in the i, j cavity modes, into the Schrödinger equation in the interaction picture and applying the Wigner-Weisskopf method [26], we obtain the integro-differential equation for the parametric interaction of modes p and s with eigenfrequencies ω_p, ω_s, corresponding to the MDR distance $\omega_{ps} = |\omega_p - \omega_s|$ [11]:

$$\dot{C}_s(t) = -n_p(n_s+1)V\gamma_s \int_0^\infty d\omega (S_{ps}^{(n)})^2 \rho(\omega) L(\omega - \omega_s, \Gamma) G(t,\omega). \tag{11}$$

Here n_p, n_s are the respective photon numbers, γ_s is the ω_s-mode linewidth, $\rho = m^3\omega^2/(\pi^2 c^3)$ denotes the free-space density of states, and $L(\omega - \omega_s, \Gamma)$ is a Lorentzian centered at ω_s, Γ being the homogeneous linewidth of the Raman process. The last factor in the integral of Eq. (11) is

$$G(t,\omega) = \int_0^t C_s(t') \exp\{[i(\omega - \omega_{ps}) - \gamma_s](t - t')\} dt. \tag{12}$$

Analogous equations are obtainable for $\dot{C}_p$, upon replacing the indices $s \leftrightarrow p$. We shall assume in what follows that the pump field is intense and undepleted, as opposed to the Stokes field. The factor n_p in Eq. (11) leads to the expected linear dependence of the transition rate on the laser intensity, while the factor $n_s + 1$ leads to stimulated scattering through the contribution of n_s and to spontaneous scattering through the contribution of unity. This dependence is reminiscent of the stimulated and spontaneous contributions to the single-photon emission rate of an atom, as described by the Einstein A and B coefficients [27].

Equations (11) and (12) yield multiexponential damping at times long enough for the oscillation in Eq. (12) to subside. The resulting solution for $C_s(t)$ will be written under the following conditions: (1) $\Gamma \gg \gamma_{s,p}$, which is appropriate for high-Q modes of the resonator; (2) we single out two interacting modes within the homogeneous Γ width, one being the pump mode and the other the resonant signal (Stokes) mode—namely, both the input and the output resonance conditions hold [4,16]. The input resonance condition is satisfied for a broadband input pump, which spans several high-Q MDR's, whereas the output resonance condition is always satisfied, since the bandwidth of Raman scattering spans at least several high-Q MDR's. The high-Q modes modulate the free-space mode density $\rho(\omega)$ by sharp Lorentzian peaks. Near ω_s, the relevant Lorentzian has width γ_s. We then obtain, from Eqs. (11) and (12) [11],

$$C_s(t) = (p_{1,s} - p_{2,s})^{-1}[p_{1,s}\exp(-p_{1,s}t) + p_{2,s}\exp(-p_{2,s}t)], \tag{13}$$

where $p_{1,s}$ and $p_{2,s}$ are the roots of the secular equation

$$p_s(p_s + \gamma_s - i\xi) + \beta_s = 0, \tag{14}$$

with $\xi = \omega_p - \omega_{ps} - \omega_s$ and

$$\beta_s = (S_{ps}^{(n)})^2 n_p(n_s+1)\gamma_s V\rho_s\omega_s\Gamma^{-1}. \tag{15}$$

The Raman transition rate will be evaluated for the two-photon resonant case $\xi = 0$. In the underdamped limit $\beta_s \gg (\gamma_s/2)^2$, we obtain $p_{1,2} = \gamma_s/2 \pm i\beta_s^{1/2}$. In this limit there is an oscillatory modulation of the Raman decay rate at the frequency $\beta_s^{1/2}$. We shall be concerned with the overdamped limit $(\gamma_s/2)^2 \gg \beta_s$, yielding $|p_{1,s}| \approx \beta_s/\gamma_s$. The condition for Raman amplification inside a cavity is that the corresponding Raman rate $|p_s|$ be greater than the transverse relaxation rate of the model, given here by the homogeneous Raman linewidth Γ. The threshold of Raman amplification is then determined by

$$\Gamma = |p_s| = \beta_s/\gamma_s. \tag{16}$$

This threshold condition implies, using Eq. (15), that the threshold numbers of photons in the p and s modes are

$$n_p\,(n_s+1)|_{th} = \frac{3\Gamma^2}{\rho_s V\omega_s (S_{ps}^{(n)})^2}. \tag{17}$$

The corresponding occupation photon number n_p in the p mode inside the resonator in the spontaneous regime of amplification, when $n_s \ll 1$, has the form

$$n_p^{spo}|_{th} = \frac{3\omega_p\Gamma^2}{\rho_s V\omega_s (S_{ps}^{(n)})^2}. \tag{18}$$

In order to obtain the Raman gain we use the rate equation for the occupation number of photons in the p and s modes [9]:

$$\frac{dn_s}{dt} = Dn_p(n_s+1). \tag{19}$$

Here D is the rate constant, determined as follows in the spontaneous regime $n_s \ll 1$: one photon from the p mode is lost for each Stokes photon that is created. Hence, the cavity enhanced decay rate β_s/γ_s in Eqs. (15) and (16) corresponds to the spontaneous rate

$$D_{spo} = \frac{\rho_s V\omega_s (S_{ps}^{(n)})^2}{\Gamma}. \tag{20}$$

The Stokes intensity in the spontaneous regime is proportional to the effective amplification length l_{eff} in the spherical resonator, traversed at the velocity c/m during the photon lifetime in the mode, yielding [28]

$$n_s|_{spo} = \frac{m}{c} D_{spo} n_p l_{eff}. \tag{21}$$

The Raman gain per unit length in the spontaneous amplification regime is correspondingly

$$G^{spo} = \frac{D_{spo} m n_p}{c}. \tag{22}$$

The total gain scales with l_{eff}, which can be expressed via the Q factor of the p mode:

$$l_{eff} = 2cQ_p / m\omega_p, \tag{23}$$

where

$$\frac{1}{Q_p} = \left(\frac{1}{Q_{scat}} + \frac{1}{Q_{abs}}\right)_p, \tag{24}$$

$(Q_{scat})_p$ and $(Q_{abs})_p$ being the Q factors of scattering loss and absorption loss in the p mode. We can now derive the threshold incident intensity P_{th}^{sp} of the pump for spontaneous Raman amplification using the basic relation for any Q factor [29]—namely, that a Q factor is the ratio of the field energy inside the mode to the incident power, multiplied by the leakage rate. This yields, at threshold,

$$Q_p = \frac{\pi\hbar\omega_p^2 n_p^{spo}|_{th}}{P_{th}^{spo}\sigma_{ext} Q_p}, \tag{25}$$

where $n_p^{spo}|_{th}$ is given by Eq. (18) and σ_{eff} is the extinction cross section of the p mode. The threshold incident intensity of the pump for spontaneous Raman amplification is then obtained from Eqs. (18)–(21), yielding

$$P_{th}^{spo} = \frac{3\pi\hbar\omega_p^2\Gamma^2}{\sigma_{ext}Q_p^2\rho_s V\omega_s (S_{ps}^{(n)})^2}, \tag{26}$$

σ_{ext} being the extinction cross section of the pump mode. The threshold intensity of the incident laser pump is thus inversely proportional to the coupling of partial modes squared, $(S_{ps}^{(n)})^2$, and to the Q factor of the pump mode squared.

It is advantageous to relate the gain coefficient for spontaneous Raman amplification to the extinction (scattering) cross section σ_{ext}. Using formulas (22)–(26), we obtain, for the gain normalized to the threshold intensity pump,

$$G_{norm}^{spo} = \frac{G^{spo}}{P_p|_{th}^{spo}} = \frac{2mQ_p(\rho_s V\omega_s)(S_{ps}^{(n)})^2\sigma_{ext}}{3c\hbar\omega_p^2\Gamma}. \tag{27}$$

The useful new results (26) and (27) allow us to relate the threshold and gain relevant experimental parameters.

In order to obtain the threshold intensity of stimulated Raman amplification in the limit $n_s \gg 1$, we employ the Manley-Rowe (energy-conservation) condition, relating the numbers of Stokes and pump photons [9,22]:

$$n_s|_{st} = \left(\frac{\omega_p Q_s}{\omega_s Q_p}\right) n_p. \tag{28}$$

The threshold intensity of stimulated amplification, derived analogously to Eq. (21) for n_p, $n_s \gg 1$, is then

$$P_{th}^{st} = \frac{3^{1/2}\pi\hbar\omega_p^2\Gamma}{\sigma_{ext}Q_p^2(\omega_p\rho_s V)^{1/2}(S_{ps}^{(n)})^2}\left(\frac{Q_p}{Q_s}\right)^{1/2}. \tag{29}$$

The threshold p-mode gain per s-mode photon can be introduced by means of Eqs. (17) and (18) and yields the rate constant

$$D_{st} = \frac{Q_s\rho_s V\omega_p(S_{ps}^{(n)})^2}{Q_p\Gamma}. \tag{30}$$

The stimulated Raman gain normalized to the threshold intensity (29) is found to be

$$G_{norm}^{st} = \frac{G^{st}}{P_{th}^{st}} = \frac{mQ_s\rho_s V(S_{ps}^{(n)})^2\sigma_{ext}}{c\Gamma\hbar\omega_p}. \tag{31}$$

The threshold intensity $P_{th}^{spo,st}$ of p-mode excitation as well as the Raman scattering cross section σ_R is obtained from experimental data [9,22]. Thus, using Eq. (25) or (29), we have an effective tool for measuring the concentration of Raman active molecules N in the form

$$N = \frac{G_{norm}^{spo,st}P_{th}^{spo,st}}{\sigma_R}. \tag{32}$$

In Secs. III and IV we explicitly evaluate the factors $G_{norm}^{spo,st}$ in nonlinear spheres.

C. Parametric amplification threshold in three- and four-wave mixing

In this subsection, we consider the threshold and gain for parametric amplification or parametric down-conversion, which are described in the interaction picture by Hamiltonian (8). The signal and idler modes at frequencies ω_s and ω_i, respectively, are coupled via a coefficient proportional to the second- $(n=2)$ or third- $(n=3)$ order nonlinearity and to the pump-mode amplitude or intensity A_p^{n-1}, for $n=2$ or $n=3$, respectively. The signal and idler modes will be quantitized and the p mode will be treated classically. Substituting the photon state $|\Psi\rangle = \Sigma_{n_s,n_i} C_{n_s,n_i}|n_s,n_i\rangle$, with n_s, n_i photon numbers in the s, i cavity modes, into the Schrödinger equation and applying the Wigner-Weisskopf method [30], we obtain the integro-differential equation for parametric interaction of the s and i modes:

$$\dot{C}_s(t) = -(n_s+1)(n_i+1)V(A_p^{n-1})^2\int_0^\infty d\omega (S_{is}^{(n)})^2\rho_i(\omega) \times \gamma_i L(\omega-\omega_i,\gamma_i)G(t,\omega), \tag{33}$$

with parameters defined analogously to those in Eq. (11) and the factor $G(t,\omega)$ described by Eq. (12). Following the same procedure as that leading to Eq. (13), we obtain the following equation for $C_s(t)$ in the Weisskopf-Wigner approximation [26,30]:

$$\dot{C}_s(t) = -\eta C_s, \tag{34}$$

where

$$\eta = (n_s + 1)(n_i + 1)\rho_i V \omega_i (A_p^{n-1} S_{is}^{(n)})^2 \gamma_i^{-1}. \quad (35)$$

We note that this approximation is valid in the limits $(S_{is}^{(n)})^2 \gamma_i^{-1} \ll 1$, $(A_p^{n-1})^2 \gg 1$, $(S_{is}^{(n)})^2 \gamma_i^{-1} (A_p^{n-1})^2 = \text{const}$. The threshold of parametric amplification is then determined from Eq. (35) by

$$\eta = \gamma_s. \quad (36)$$

This threshold condition implies that the threshold occupation numbers for s and i modes are

$$(n_s + 1)(n_i + 1)\big|_{th} = \frac{\gamma_s \gamma_i}{\rho_i V \omega_i (A_p^{n-1} S_{is}^{(n)})^2}. \quad (37)$$

In the case of spontaneous down-conversion we have from Eq. (37) the threshold condition

$$\rho_i V \omega_i (A_p^{n-1} S_{ik}^{(n)})^2 = \gamma_s \gamma_i. \quad (38)$$

Analogously to Eq. (19), we can obtain the rate constant D in the spontaneous limit $n_{s,i} \ll 1$ in the form

$$D_{spo} = \frac{\rho_i V \omega_i (S_{is}^{(n)})^2}{\gamma_i} (A_p^{n-1})^2. \quad (39)$$

For the stored threshold energy in the modes s and i in the degenerate case of stimulated amplification $(\omega_s = \omega_i)$, in the limit of $n_i \gg 1$ and $n_s \gg 1$, we obtain

$$W_s = \left(\frac{\gamma_s \gamma_i}{\rho_i V \omega_i} \right)^{1/2} \frac{\hbar \omega_s}{A_p^{(n-1)} S_{is}^{(n)}}. \quad (40)$$

Using formulas (25), (28), and (37), we have, for the threshold intensity of laser pump,

$$P_{th} = \frac{2\pi \hbar \omega_p \omega_s}{\sigma_{ext} Q_p Q_s} \left(\frac{\gamma_p \gamma_i}{\rho_i V \omega_i} \right)^{1/2} \frac{1}{A_p^{n-1} (S_{is}^{(n)})}. \quad (41)$$

Taking into account that the number of pump photons converted to two photons in the signal and idler modes satisfies $2n_p = n_i + n_s$ in $\chi^{(3)}$ media or $n_p = n_i + n_s$ in $\chi^{(2)}$ media, and the basic relation for the Q factor (Sec. II B), we can obtain the following formula for the gain of stimulated amplification normalized to the pump intensity:

$$G_{norm} = \frac{G^{st}}{P_p} = \frac{2m(\rho_i V \omega_i) A_p^2 (S_{is}^{(2)})^2 \sigma_{ext}}{c \hbar \omega_p \gamma_i \gamma_p} \quad (42)$$

for $(n=2)$ and

$$G_{norm} = \frac{G^{st}}{P_p} = \frac{2m(\rho_i V \omega_i) A_p^4 (S_{is}^{(3)})^2 \sigma_{ext}}{c \hbar \omega_p \gamma_i \gamma_p} \quad (43)$$

for $(n=3)$.

III. INTEGRAL COEFFICIENTS AND INTERACTING MODES

In this section we pursue the calculation of the coupling between interacting electromagnetic modes and the selection rules governing this coupling. Integral coefficients of coupling between modes in a microsphere in Hamiltonians (7) and (8) may be written as [21]

$$S_{ij}^{(2)} = \frac{b_k (\omega_i \omega_j)^{1/2}}{6m^2} C_{ijk}^{(2)} \quad (44)$$

and

$$S_{ij}^{(3)} = \frac{b_k b_q (\omega_i \omega_j)^{1/2}}{2m^2} C_{ijkq}^{(3)} \quad (45)$$

for second- and third-order nonlinearities, respectively, where b_k are given by Eq. (A5) or (A6) and $C_{ijk}^{(2)}$ and $C_{ijkq}^{(3)}$ are the volume integrals,

$$C_{ijk}^{(2)} = \chi_{ijk}^{(2)} \int_V \vec{E}_i(\vec{r}) \vec{E}_j(\vec{r}) \vec{E}_k(\vec{r}) dV, \quad (46)$$

with $\chi_{ijk}^{(2)} = \chi^{(2)}(\omega_i + \omega_j = \omega_k)$ or permutations thereof [21],

$$C_{ijkq}^{(3)} = \chi_{ijkq}^{(3)} \int_V \vec{E}_i(\vec{r}) \vec{E}_j(\vec{r}) \vec{E}_k(\vec{r}) \vec{E}_q(\vec{r}) dV, \quad (47)$$

and with $\chi_{ijkq}^{(3)} = \chi^{(3)}(\omega_i, -\omega_i, \omega_k, -\omega_k)$ or permutations thereof. Under input-output resonance conditions, only $\omega_i = \omega_s$ and $\omega_k = \omega_p$ differ from each other, while $\omega_j = \pm \omega_s$, $\omega_q = \pm \omega_p$. These integrals are separable into radial and angular parts. The scalar form is

$$\int_V E_{ai} E_{bj} E_{ck} dV = \int_0^{r_0} R_{ai}(k_i r) R_{bj}(k_j r) R_{ck}(k_k r) r^2 dr \times \int_0^{\pi} \Theta_{ai}(\theta) \Theta_{bj}(\theta) \Theta_{ck}(\theta) sin(\theta) d\theta \times \int_0^{2\pi} \exp i(m_{ai} + m_{bj} + m_{ck}) d\varphi \quad (48)$$

for $C_{ijk}^{(2)}$ and

$$\int_V E_{ai} E_{bj} E_{ck} E_{dq} dV = \int_0^{r_0} R_{ai}(k_i r) R_{bj}(k_j r) R_{ck}(k_k r) R_{dq}(k_q r) r^2 dr \times \int_0^{\pi} \Theta_{ai}(\theta) \Theta_{bj}(\theta) \Theta_{ck}(\theta) \Theta_{dq}(\theta) sin(\theta) d\theta \times \int_0^{2\pi} \exp i(m_{ai} + m_{bj} + m_{ck} + m_{dq}) d\varphi \quad (49)$$

for $C_{ijkq}^{(3)}$. Here the indices i,j,k,q correspond to the principal mode numbers whereas a,b,c,d label the polar index r and azimuthal indices θ and φ of either the TE or TM mode. The well-known angular parts of the eigenfunctions of TE and TM modes Θ_{ai}, Θ_{bj}, Θ_{ck}, and Θ_{dq} and the corresponding resonant size parameters are given in the Appendix. In order to calculate the integral coefficients in Eqs. (9) and (10), we have developed numerical (FORTRAN) algorithms that evaluate the radial part of the integral coefficients by Simpson methods of integration, the angular part involving Clebsch-Gordan integrals, and the associated Legendre polynomials

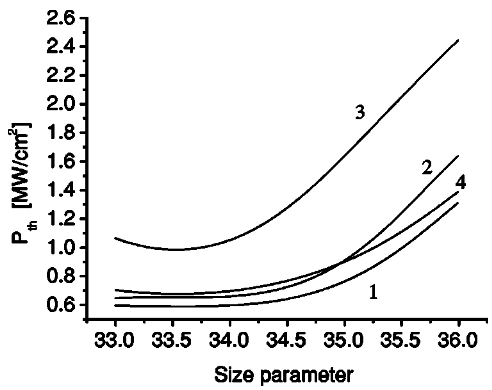

FIG. 1. The threshold intensity for spontaneous Raman scattering from fused silica microsphere irradiated by laser pump of wavelength 840 nm. 1, $TE^0_{42}-TE^1_{45}$. 2, $TE^0_{42}-TE^1_{44}$; 3, $TE^0_{42}-TE^1_{43}$; 4, $TE^0_{42}-TE^1_{42}$.

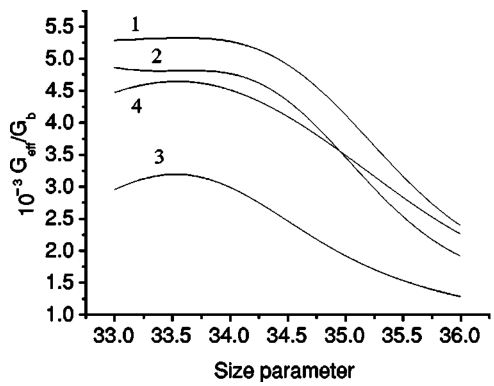

FIG. 2. The cavity enhanced gain normalized to its value in bulk for the same process as Fig. 1. 1, $TE^0_{42}-TE^1_{45}$; 2, $TE^0_{42}-TE^1_{44}$; 3, $TE^0_{42}-TE^1_{43}$; 4, $TE^0_{42}-TE^1_{42}$.

by the Gauss-Hermite and Tschebishev methods. The Riccati-Bessel, spherical Bessel, and Neumann functions were calculated by well-known recurrence methods. With such algorithms we were able to perform the calculation up to size parameter 170 and mode number $n=170$. The most appreciable couplings involve two modes of the form $TE^m_n - TM^m_n$, $TE^m_n - TE^m_n$, and $TM^m_n - TM^m_n$, traveling inside the microsphere near the surface.

The integral coefficients for such pairs of modes differ from zero only in the case of phase factor $\exp(\pm\Sigma_i m_{ai}\varphi) \neq 0$. This yields the following selection rule for a sphere with second-order nonlinearity in the form

$$|m_{ai} \pm m_{bj} \pm m_{ck}| = 0. \tag{50}$$

For the two-mode $\chi^{(2)}$-nonlinear interaction this implies $m_p = 2m_s$. For a sphere with third-order nonlinearity,

$$|m_{ai} \pm m_{bj} \pm m_{ck} \pm m_{dl}| = 0, \tag{51}$$

which implies for two-mode interaction $m_p = m_s$. The addition rules of orbital momenta $\vec{\ell}_{ai} \pm \vec{\ell}_{bj} \pm \vec{\ell}_{ck}$ are more complicated [25]. These rules, allowing us to select interacting modes, are alternative to the phase-matching or selection rules for the same processes in bulk or in planar cavities [9].

IV. RESULTS

We may now quantitatively consider the dependence of the threshold intensity of the spontaneous and stimulated amplification on the size parameter and numbers of interacting modes. In Figs. 1 and 2 the spontaneous Raman threshold intensity [Eq. (26)] and gain [Eq. (27)] are presented for pairs of modes obeying the selection rules of Sec. III. To be specific, here we concentrate on the threshold intensity of spontaneous Raman scattering and the threshold of stimulated Brillouin scattering (SBS) for modes whose amplitudes and resonance half-widths are given in [31]. The threshold pump intensity for spontaneous Raman scattering [Eq. (26)] is found to be 0.6 MW/cm^2, well below the threshold of stimulated Brillouin scattering in a glass sphere, which is of order 9.5 MW/cm^2. The threshold intensity calculated by us for mode-locked $Ti:Al_2O_3$ laser pump operating at 840 nm for particle sizes between 1.5 and 5 μm ranges from 0.3 to 2.6 MW/cm^2. This finding is in agreement with the experiments of high-Q-factor dielectric resonators such as spherical aerosol droplets, where the output signal from the particle was 10^3 times larger than the signal from the bulk [32], as explained by the gain presented below. The different thresholds and interacting modes involved allow us to separate these nonlinear processes from each other.

Nonlinear stimulated and spontaneous thermal scattering has yet another threshold intensity [33]. Its measurement may allow us to infer the temperature of the droplets or microspheres. The microsphere-enhanced gain in nonlinear spheres [Eq. (27)] with the size parameter $33 \leqslant \rho \leqslant 36$ can be three orders of magnitude higher than the gain of silica bulk [9]. In Figs. 3 and 4, the threshold intensities and gain for stimulated Raman scattering are presented in dependence on the MDR number. The threshold intensity for stimulated Raman amplification in Er:Yb-doped phosphate glass microspheres with diameter 57 μm irradiated by laser pump at 1.06 μm is found to be very small, of order 10 W/cm^2 or even less. The gain of stimulated amplification [Eq. (31)] can be dramatically enhanced relative to its counterpart in bulk by 3.5×10^4 times.

For stimulated parametric amplification or parametric down-conversion we have calculated the spontaneous thresh-

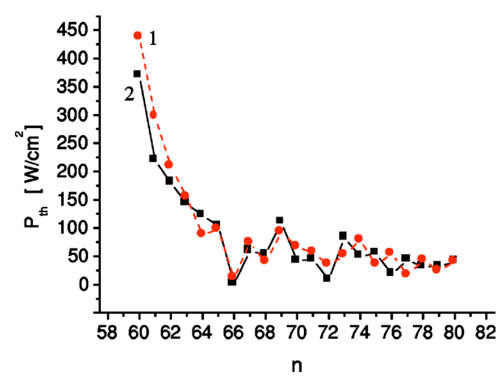

FIG. 3. The threshold of stimulated Raman amplification for Er:Yb-doped phosphate glass microsphere (diameter of 57 μm) for different MDR orders n: 1, $TE^0_{2n}-TE^1_{2n}$ modes; 2, $TE^0_{2n}-TE^1_{2n+1}$ modes. The laser pump has the wavelength 1.06 μm.

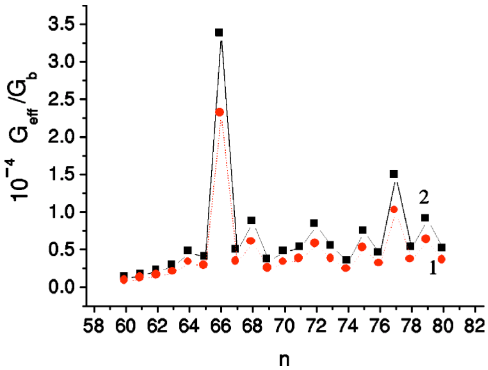

FIG. 4. The stimulated cavity-enhanced gain normalized to its bulk value for the same process and modes as in Fig. 3.

old intensity [Eqs. (39)–(41)] and effective stimulated gain [Eqs. (42) and (43)] normalized to gain in bulk of the same substance in dependence on the MDR order n (Figs. 5 and 6). The interacting degenerate modes TE^1_{2n} and TE^2_{2n} are coupled by a laser pump at a wavelength of 840 nm in a nonlinear SiO_2 sphere with diameter 57 μm and $\chi^{(2)}=0.96\times10^{-9}$ esu [9,21]. Remarkably, there are MDR mode numbers where the threshold intensity of parametric downconversion decreases with increasing MDR number, but the normalized gain tends to grow. In the region of MDR's with $40\leqslant n\leqslant 80$ for TE^1_{2n}, the threshold intensity is approximately 1 MW/cm^2 and the normalized gain is 20. Compared to the threshold intensity of Raman amplification in Fig. 3, the threshold intensity of parametric downconversion is considerably higher for the same MDR order. Correspondingly, the normalized gain of parametric downconversion is significantly lower than the normalized gain of stimulated Raman amplification.

V. DISCUSSION

The unified theory of spontaneous and stimulated Raman and parametric amplification has been developed with an explicit analysis of microspherical nonlinear cavities. We have theoretically considered the decrease of the threshold intensity and increase of the gain under conditions of input and output resonances, satisfied by nonlinearly coupled modes near morphology dependent resonances (MDR's). Our approach is based on the expansion of the internal field of the coupled modes in the basis of eigenfunctions of the stationary diffraction problem, yielding their internal partial-wave amplitudes. The coupling of these partial waves has been accounted for by the integral coefficients, associated with second- or third-order nonlinearity. It has been shown that in the amplification of Stokes modes or in three- and four-wave mixing, the threshold of excitation and gain can reveal the concentration of the active molecules.

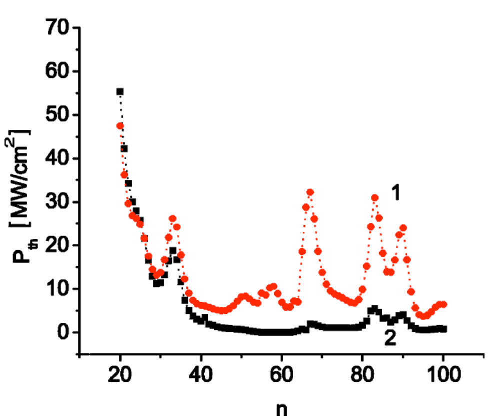

FIG. 5. The threshold intensity of stimulated parametric amplification for microsphere from fused silica (SiO_2) irradiated by laser light with wavelength (840 nm), with the interacting degenerate modes. 1, $TE^2_{2n}-TE^2_{2n}$; 2, $TE^1_{2n}-TE^1_{2n}$.

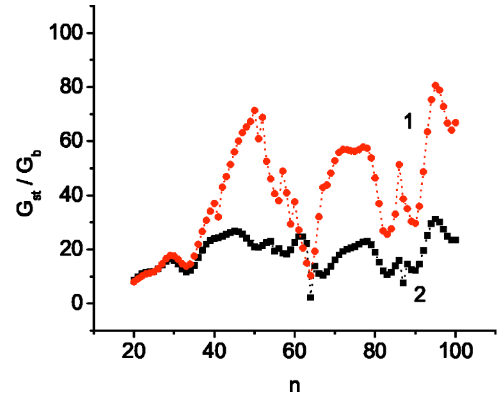

FIG. 6. The cavity-enhanced gain normalized to its bulk value for the same process and modes.

Various applications of the foregoing results are foreseen:

(1) Measurements of the stimulated threshold may be used to estimate the concentration of Raman-active molecules or nanoparticles (inclusions) embedded in microspherical resonators or aerosol droplets.

(2) Alternatively, they could be used for experimental estimation of Q factors, temperature, and $\chi^{(2)}$ and $\chi^{(3)}$ nonlinear permeability.

(3) The enormous enhancement of gain, by three or four orders of magnitude, suggests applications in the context of nonlinear optical microscopy, based on Raman amplification.

(4) The ultralow thresholds of stimulated Raman amplification in the two-mode regime, typically less than 10 W/cm^2, may lead to the development of optical microamplifiers based on solid spheres and on aerosol droplets in a wide range of wavelengths. Glass spheres with Raman-active inclusions may act as high-gain and low-threshold Raman amplifiers with THz Stokes shift, pumped by sunlight or laser radiation.

(5) We find that the thresholds of parametric downconversion in silica microspheres are amenable to experimental observation, because this threshold is significantly lower than the threshold of optical discharge in the substance. Furthermore, we may assume that the normalized gain can be increased using the excitation of partial waves of higher order.

(6) Raman amplification may be used for atmospheric aerosol identification by providing information on the surface concentration of any chemical substances, from the threshold intensity of the nonlinear scattering processes.

(7) The surface mode pairs with strong nonlinear coupling have very low thresholds and large gain. As was shown in

[34] there is a line broadening of the modes with size parameters $33 \leqslant \rho \leqslant 36$ if the microsphere is doped with latex nanoparticles. The concentration of any absorbing or scattering nanoparticles could be estimated by formula (34). The threshold for Raman amplification will increase due to losses incurred by absorbing nanoparticles. However, if the nanoparticles are nonabsorbing, the effect of line broadening may keep the Q factors intact and cause the splitting of resonant modes. In this case the integral coefficients of the interaction between "split" Stokes and pump (or signal and idler) modes may actually increase. This intriguing possibility calls for further investigation, whose practical aim may be the creation of broadband microsphere amplifiers.

ACKNOWLEDGMENTS

We acknowledge the support of the EU (through the ATESIT and QUACS Networks), ISF, and Minerva.

APPENDIX: PARTIAL-WAVE AMPLITUDES AND EIGENMODES OF SPHERICAL-MORPHOLOGY-DEPENDENT RESONANCES

For the radial and angular parts of TM-mode eigenfunctions we have [12]

$$R_{\theta i}(k_i r) = -\frac{1}{(k_i r)}\psi_n(k_i r),$$

$$R_{\varphi i}(k_i r) = -\frac{1}{(k_i r)}\psi_n(k_i r),$$

$$\Theta_{\theta i}(\theta) = \frac{im}{\sin(\theta)}P_n^{(m)\prime}[\cos(\theta)],$$

$$\Theta_{\varphi i}(\theta) = P_n^{(m)\prime}(\cos\theta)\sin(\theta), \qquad \text{(A1)}$$

and for their TE-mode counterparts

$$R_{ri}(k_i r) = \frac{-n(n+1)}{(k_i r)^2}\psi_n(k_i r),$$

$$R_{\theta i}(k_i r) = \frac{1}{(k_i r)}\psi_n'(k_i r),$$

$$R_{\varphi i}(k_i r) = \frac{1}{(k_i r)}\psi_n(k_i r),$$

$$\Theta_{ri}(\theta) = P_n^{(m)}[\cos(\theta)],$$

$$\Theta_{\theta i}(\theta) = P_n^{(m)\prime}[\cos(\theta)]\sin(\theta),$$

$$\Theta_{\varphi i}(\theta) = \frac{im}{\sin(\theta)}P_n^{(m)}(\cos\theta). \qquad \text{(A2)}$$

Here $\psi_n(k_i r)$ and $\psi_n'(k_i r)$ are the first-kind Riccati-Bessel functions and their derivatives, respectively; $P_n^{(m)}[\cos(\theta)]$ and $P_n^{(m)\prime}[\cos(\theta)]$ are the Legendre polynomials and their derivatives, respectively. The resonant size parameter at an MDR $\rho = k_i r_0$ may be calculated from the transcendental eigenvalue equations

$$m\xi_n(k_i r_0)\psi_n'(mk_i r_0) - \psi_n(mk_i r_0)\xi_n'(k_i r_0) = 0, \qquad \text{(A3)}$$

$$\xi_n(k_i r_0)\psi_n'(mk_i r_0) - m\psi_n(mk_i r_0)\xi_n'(k_i r_0) = 0, \qquad \text{(A4)}$$

for TE and TM modes, respectively. The partial-wave amplitudes of the Mie-scattering problem can be presented in the form [12]

$$b_n^{\mathrm{TM}} = \frac{i}{\xi_n(\rho)\psi_n'(m\rho) - m\psi_n(m\rho)\xi_n'(\rho)} \qquad \text{(A5)}$$

and

$$b_n^{\mathrm{TE}} = \frac{i}{m\xi_n(\rho)\psi_n'(m\rho) - m\psi_n(m\rho)\xi_n'(\rho)}, \qquad \text{(A6)}$$

where $\xi_n(k_i r)$ and $\xi_n'(k_i r)$ are the third-kind Riccati-Bessel functions and their derivatives, respectively. The normalizing factor for a TE mode is given in the form [12]

$$\|E^{\mathrm{TE}}\|^2 = 2\pi\frac{n(n+1)}{(2n+1)^2}\frac{(n+m)!}{(n-m)!}\left(\frac{\pi r_0^3}{4\rho}\right)\{(n+1)[J_{n-1/2}'(\rho)]^2 + n[J_{n+3/2}'(\rho)]^2\}, \qquad \text{(A7)}$$

and its counterpart for a TM mode has the form

$$\|E^{\mathrm{TM}}\|^2 = 2\pi\frac{n(n+1)}{(2n+1)^2}\frac{(n+m)!}{(n-m)!}\left(\frac{\pi r_0^3}{4\rho}\right)\{(n+1)[J_{n+1/2}'(\rho)]^2\}, \qquad \text{(A8)}$$

where $J_{n+1/2}'(\rho)$ is the derivative of the appropriate Bessel function and r_0 is the radius of the sphere.

The Q factor of each mode can be calculated in the form [29]

$$Q_j^{TM} = \frac{\pi}{4}\left\{\left[j^2\left(m^2 - \frac{1}{m^2}\right) - \frac{j}{m^2} + j\right]N_{j+1/2}^2(\rho) + \rho^2(m^2-1)N_{j-1/2}^2(\rho)\right\} - \frac{\pi}{4}[2j\rho(m^2-1)N_{j+1/2}(\rho) \times N_{j-1/2}(\rho) + (j-\rho^2)J_{j+1/2}^2(\rho)] - \frac{\pi}{4}\left[\rho^2 J_{j-1/2}^2(\rho) + 2j\rho J_{j+1/2}(\rho)J_{n-1/2}(\rho) + \frac{4}{\pi}\rho\right] \qquad \text{(A9)}$$

and

$$Q_j^{\mathrm{TE}} = \frac{\pi}{4}[\rho^2(m^2-1)N_{j+1/2}^2(\rho)(j-\rho^2)J_{j+1/2}^2(\rho)] - \frac{\pi}{4}\left[\rho^2 J_{j-1/2}^2(\rho) + 2j\rho J_{j+1/2}(\rho)J_{n-1/2}(\rho) + \frac{4}{\pi}\rho\right], \qquad \text{(A10)}$$

where $N_j(\rho)$ is the Neumann function.

[1] P. Barber and R. Chang, *Optical Effects Associated with Small Particles* (World Scientific, Singapore, 1988).
[2] P. Barber and S. Hill, *Light Scattering by Particles: Computational Methods* (World Scientific, Singapore, 1990).
[3] J. Eversole, H. Lin, and A. Campillo, J. Opt. Soc. Am. B **12**, 287 (1995).
[4] S.-X. Quian, J. Snow, and R. Chang, Opt. Lett. **10**, 499 (1985).
[5] S. Quian and R. Chang, Phys. Rev. Lett. **56**, 926 (1989).
[6] A. Campillo, J. Eversole, and H.-B. Lin, Phys. Rev. Lett. **67**, 437 (1991).
[7] G. Kurizki and A. Nitzan, Phys. Rev. A **38**, 267 (1988).
[8] H.-B. Lin and A. Campillo, Phys. Rev. Lett. **73**, 2440 (1994).
[9] R. Boyd, *Nonlinear Optics* (Academic Press, Boston, 1984).
[10] H. Lai, P. Leung, and K. Young, Phys. Rev. A **37**, 1597 (1988).
[11] Y. Wu, X. Yang, and P. Leung, Opt. Lett. **24**, 345 (1999).
[12] J. Stratton, *Electromagnetic Theory* (McGraw-Hill, New-York, 1941).
[13] G. Roll, T. Kaiser, and G. Schweiger, J. Opt. Soc. Am. A **16**, 882 (1999).
[14] A. Biswas, H. Latifi, R. Armstrong, and R. Pinnik, Phys. Rev. B **40**, 7413 (1989).
[15] D. Braunstein, A. Khazanov, G. Koganov, and R. Shuker, Phys. Rev. A **53**, 3565 (1996).
[16] G. Schweiger, J. Raman Spectrosc. **21**, 165 (1990).
[17] G. Schweiger, J. Opt. Soc. Am. B **8**, 1770 (1991).
[18] M. Gorodetsky, A. Pryamikov, and V. Ilchenko, J. Opt. Soc. Am. B **17**, 1051 (2000).
[19] H. B. Lin, A. L. Huston, J. D. Eversole, and A. J. Campillo, J. Opt. Soc. Am. B **7**, 2079 (1990).
[20] V. Braginsky, M. Gorodetsky, and V. Ilchenko, Phys. Lett. A **137**, 393 (1989).
[21] A. Yariv, *Quantum Electronics* (Wiley, New York, 1989).
[22] Y. Shen, *The Principles of Nonlinear Optics* (Wiley, New York, 1984).
[23] Y. Wu, Phys. Rev. A **54**, 1586 (1996).
[24] Y. Wu and X. Yang, Opt. Lett. **28**, 1793 (2003).
[25] D. Varshalovich, A. Moskalev, and V. Khersonsky, *Quantum Theory of Angular Momentum* (World Scientific, Singapore, 1988).
[26] W. Heitler, *Quantum Theory of Radiation* (Oxford University Press, New York, 1949).
[27] S. Ching, H. Lai, and K. Young, J. Opt. Soc. Am. B **4**, 1995 (1987).
[28] J.-Z. Zhang, D. Leach, and R. Chang, Opt. Lett. **13**, 270 (1988).
[29] P. Affolter and B. Eliasson, IEEE Trans. Microwave Theory Tech. **MTT–21**, 573 (1973).
[30] M. Scully and M. Zubairy, *Quantum Optics* (Cambridge University Press, Cambridge, England, 1997).
[31] S. M. Chitanvis and C. D. Cantrell, J. Opt. Soc. Am. B **6**, 1326 (1989).
[32] H.-B. Lin and A. Campillo, Opt. Commun. **133**, 287 (1997).
[33] M. Gorodetsky and V. Ilchenko, Laser Phys. **2**, 1004 (1992).
[34] S. Pellegrin, A. Kozhekin, A. Sarfati, V. M. Akulin, and G. Kurizki, Phys. Rev. A **63**, 033814 (2001).